

Casimir squared correction to the standard rotator Hamiltonian for the $O(n)$ sigma-model in the delta-regime

F. Niedermayer^a and P. Weisz^b

^a*Albert Einstein Center for Fundamental Physics,
Institute for Theoretical Physics, University of Bern, Switzerland*

^b*Max-Planck-Institut für Physik, 80805 Munich, Germany*

E-mail: niedermayer@itp.unibe.ch, pew@mpp.mpg.de

ABSTRACT: In a previous paper we found that the isospin susceptibility of the $O(n)$ sigma-model calculated in the standard rotator approximation differs from the next-to-next to leading order chiral perturbation theory result in terms vanishing like $1/\ell$, for $\ell = L_t/L \rightarrow \infty$ and further showed that this deviation could be described by a correction to the rotator spectrum proportional to the square of the quadratic Casimir invariant. Here we confront this expectation with analytic nonperturbative results on the spectrum in 2 dimensions, by Balog and Hegedüs for $n = 3, 4$ and by Gromov, Kazakov and Vieira for $n = 4$. We also consider the case of 3 dimensions.

Contents

1	Introduction	1
2	The isospin susceptibility	3
3	Delta regime in $d = 2$	5
3.1	Running coupling functions	8
3.2	The Balog-Hegedüs results for the $I = 1, 2$ energies for $O(3)$	9
3.3	The $O(4)$ case	10
4	The case $d = 3$	12
5	Acknowledgements	14
A	Spectrum of $O(3)$ rotator in $d = 1$ at finite lattice spacing	14
B	The sunset diagram for $D \sim 2, 3, 4$ for large ℓ	15
B.1	Case $D \sim 2$	15
B.2	Case $D \sim 3$	16
C	The equations for the lowest energy state in a finite volume for the vacuum, 1- and 2-particle sectors	17
C.1	The iterative calculation of the vacuum energy	18
C.2	Using discrete FT	19
C.3	N -dependence of the sums appearing in FT and the Euler-Bernoulli relation	20
C.4	The energy of the 1-particle sector	21
C.5	The ground state energy of the 2-particle sector	21

1 Introduction

In the pioneering paper [1] Leutwyler showed that to lowest order in chiral perturbation theory (χ Pt) the low energy dynamics of QCD in the δ -regime is described by a quantum rotator for the spatially constant Goldstone modes. We recall that for a system in a periodic spatial box of sides L the δ -regime is where the time extent $L_t \gg L$ and $m_\pi L$ is small (i.e. small or zero quark mass) whereas $F_\pi L$, (F_π the pion decay constant) is large.

There are other important physical systems, in particular in condensed matter physics where anti-ferromagnetic layers are described by the $O(3)$ sigma-model for $d = 3$ [2], where the order parameter of the spontaneous symmetry breaking is an $O(3)$ vector. In the analogous perturbative regime these systems and also the non-linear sigma models in $d = 2$ are described by a quantum rotator to leading order.

In all such systems the lowest energy momentum zero states of isospin I have to leading order χ PT energies of the form

$$E_I \propto \mathcal{C}_{n;I}, \quad (1.1)$$

where

$$\mathcal{C}_{n;I} = I(I + n - 2), \quad (1.2)$$

is the eigenvalue of the quadratic Casimir for isospin I .

At 1-loop level it turns out that the Casimir scaling (1.1) still holds, but it is of course expected that at some higher order the standard rotator spectrum will be modified. The standard rotator describes a system where the length of the total magnetization on a time-slice does not change in time. This is obviously not true in the full effective model given by χ PT. To our knowledge, the actual deviation from the Casimir scaling was first observed by Balog and Hegedüs [3] in their computation of the spectrum of the $d = 2$ O(3) non-linear sigma model in a small periodic box (circle) using the thermodynamic Bethe ansatz (TBA).

Of course, a deviation from the standard rotator spectrum could be established by explicit perturbative computations. However, in our previous paper [5] we pointed out that by comparing the already obtained NNLO results for the isospin susceptibility calculated in χ PT at large $\ell \equiv L_t/L$ with that computed using the standard rotator one can establish, under reasonable assumptions, that the leading correction to the rotator Hamiltonian occurs at 3-loops and is proportional to the square of the Casimir operator with a proportionality constant determined by the NNLO LEC's of χ PT.

In Appendix A we illustrate that such corrections are expected by recalling the spectrum of the O(3) rotator in $d = 1$ with lattice regularization. Note that the appearance of terms proportional to \mathcal{C}_I^2 is not a lattice artifact. This simple example serves only to show that distorting the Lagrangian of the standard 1d rotator by an O(3) invariant perturbation leads naturally to a spectrum which (at a higher order) contains such term.

After reviewing some preliminary results in Sect. 2, in Sect. 3 we test our claim above in the $d = 2$ O(3) and O(4) non-linear sigma models in a periodic box. For O(3) we find excellent agreement of our prediction with the analytic computations of the lowest isospin 1 and 2 energies for O(3) by Balog and Hegedüs [3].

For O(4) Balog and Hegedüs [4] computed only the ground state energy; Gromov, Kazakov and Vieira [6] computed also higher state energies but the results at small volumes presented there are not sufficiently precise for our purposes. We thus generated more data; our methods used to solve the TBA equations are described in Appendix C. Again there is good agreement with our prediction.

The derivation of our result depends on the validity of a (plausible) assumption; but also there is, to our knowledge, no rigorous derivation of the TBA equations (or even the S-matrix) from first principles starting with the 2d O(n) QFT¹. Hence the agreement of the results provides extra evidence for the validity of both scenarios.

Finally in Sect. 4 compute the effect for the $d = 3$ O(n) model, but we have not yet found data for which a comparison can be made.

¹except for $n = 4$ which is also a principal chiral model

2 The isospin susceptibility

In this section we recall some results on the isospin susceptibility. The Hamiltonian of the $O(n)$ standard quantum rotator with a chemical potential coupled to the generator \hat{L}_{12} of rotations in the 12-plane is

$$H_0(h) = \frac{\hat{L}^2}{2\Theta} - h\hat{L}_{12}, \quad (2.1)$$

where Θ is the moment of inertia. In $d = 4$ dimensions to lowest order χ PT one has $\Theta \simeq F^2 L^3$. The isospin susceptibility is defined as the second derivative of the free energy wrt h :

$$\chi = \frac{1}{L_t L^{d-1}} \frac{\partial^2}{\partial h^2} \ln Z(h; \Theta) \Big|_{h=0}, \quad Z(h; \Theta) = \text{Tr} \exp\{-H_0(h)L_t\}. \quad (2.2)$$

In ref. [5] we showed that for small $u = L_t/(2\Theta)$ the isospin susceptibility computed from the standard rotator, which we call χ_{rot} is given by

$$\chi_{\text{rot}} = \frac{L_t}{nL^{d-1}u} \left[1 - \frac{1}{3}(n-2)u + \frac{1}{45}(n-2)(n-4)u^2 + \dots \right]. \quad (2.3)$$

On the other hand in a previous paper [7], we computed the isospin susceptibility in an asymmetric $L_t \times L^{d-1}$ box (with periodic boundary conditions) and the mass gap, in this case the lowest energy in the isospin 1 channel, to NNLO (next-to next-to leading order) χ PT. For the susceptibility we recall the results in eqs. (3.54)–(3.57) of [7] with dimensional regularization:

$$\chi = \frac{2}{ng_0^2} (1 + g_0^2 R_1 + g_0^4 R_2 + \dots), \quad (2.4)$$

with

$$R_1 = -2(n-2)\bar{I}_{21;D}, \quad (2.5)$$

and

$$R_2 = R_2^{(a)} + R_2^{(b)}, \quad (2.6)$$

with

$$R_2^{(a)} = 2(n-2) \left\{ -\bar{W} + 2\bar{I}_{21;D} [\bar{I}_{10;D} - \bar{I}_{21;D}] + \frac{2(n-2)}{V_D} \bar{I}_{31;D} \right\}, \quad (2.7)$$

and $R_2^{(b)}$ involves the 4-derivative couplings which we shall not include in this paper. The expressions above require some explanation. Firstly g_0 is the bare coupling for $d = 2$; $g_0^{-2} = \rho_s$, the spin stiffness for $d = 3$; and $g_0^{-2} = F^2$ for $d = 4$ where F is the pion decay constant in the chiral limit. V_D is the volume $V_D = L_t L^{D-1} \hat{\ell}^q$ where with DR we have added $q = D - d$ extra dimensions with extent $L\hat{\ell}$; in this paper we will usually set $\hat{\ell} = 1$ unless stated otherwise. (Note that the renormalized quantities do not depend on $\hat{\ell}$.) $\bar{I}_{nm;D}$ are 1-loop dimensionally regularized sums over momenta (cf eq. (3.44) of [7])². Finally \bar{W} in (2.7) is an integral associated with a two-loop vacuum massless sunset diagram, which is discussed in Appendix B.

²Note in [7] we dropped the label D and wrote only \bar{I}_{nm} .

The lowest energy state above the vacuum (the mass gap) is given by $E_1 = m_1$ in eqs. (5.9)-(5.11) of [7]:

$$E_1 = \frac{n_1 g_0^2}{2\bar{V}_D} \left[1 + g_0^2 \Delta^{(2)} + g_0^4 \Delta^{(3)} + \dots \right], \quad (2.8)$$

(here $\bar{V}_D = L^{D-1} \hat{\ell}^q$), with

$$\Delta^{(2)} = (n-2)R(0), \quad (2.9)$$

$$\Delta^{(3)} = (n-2) \left[2W + \frac{3}{4\bar{V}_D} \bar{I}_{10:D-1} + (n-3)R(0)^2 \right] + 4\text{-derivative terms}. \quad (2.10)$$

Here $R(z)$ is the propagator for an infinitely long strip without the slow modes and W is a 2-loop sunset integral discussed in Appendix B.

For the simple rotator (2.1) at zero isospin chemical potential, the energy gap is given by

$$E_1(L) = \frac{(n-1)}{2\Theta(L)}. \quad (2.11)$$

By inserting the expression for Θ using (2.8) into (2.3), we obtain the susceptibility for small u as a function of F, L, ℓ . This can then be compared to the direct χ PT computation (2.4) in the ϵ -regime for $\ell \gg 1$. The comparison requires knowledge of the large ℓ -behavior of shape functions and the sunset integral appearing in the latter, which are discussed in Appendix B of ref. [5] for $d = 4$.

The two results in NNLO differ by $\propto 1/\ell$ terms for $\ell \gg 1$, (plus terms vanishing exponentially with ℓ):

$$\frac{\chi - \chi_{\text{rot}}}{\chi} = \frac{1}{F^4 L^4} \left(\frac{\Delta_2}{\ell} + \dots \right) + \mathcal{O} \left(\frac{1}{F^6 L^6} \right), \quad (2.12)$$

for $d = 4$ and similarly for $d = 2, 3$.

In ref. [5] we showed that the deviation above can be accounted for if the spectrum to the order we are considering is given by a modified rotator with eigenvalues of the form

$$E_I(L) = \frac{1}{2\Theta(L)} \mathcal{C}_{n;I} + \frac{\Phi(L)}{L} \mathcal{C}_{n;I}^2. \quad (2.13)$$

$\Theta(L)$ appearing here contains a higher order correction with respect to the one in (2.11), denoted below by $\Theta_{\text{old}}(L)$.

$$\frac{1}{\Theta(L)} = \frac{1}{\Theta_{\text{old}}(L)} - \frac{2(n-1)}{L} \Phi(L). \quad (2.14)$$

The leading order of the coefficient $\Phi(L)$ in (2.13) is directly related to Δ_2 in (2.12). In [5] we considered only the case $d = 4$; in the next sections we consider the lower dimensions $d = 2, 3$.

It is interesting to note that the correction discussed here shows up at NNLO in the isospin susceptibility χ , and in the NNNLO (next order) in the spectrum of the effective

rotator. The reason is that in the (standard) rotator approximation the Boltzmann weight is $\sim \exp(-g^2 C_I L_t/L) = \exp(-g^2 \ell C_I)$ where $g^2 = g^2(1/L)$. The typical values of the isospin in the partition function are then given by $C_I \approx 1/(g^2 \ell)$, hence the extra factor $\exp(-C_I^2 \Phi(L) L_t/L)$ in the Boltzmann weight gives a correction $\delta\chi/\chi \sim -\Phi(L)/(g^4 \ell)$ for the susceptibility. With $\Phi(L) = \Phi_3 g^8 + \mathcal{O}(g^{10})$ (cf. [5]), the leading $\propto C_I^2$ term in the effective Hamiltonian which is of NNNLO, results in an NNLO, $\propto g^4/\ell$ term in $\delta\chi/\chi$.

3 Delta regime in $d = 2$

The susceptibility computed in χ PT is for $d = 2$ given by (cf eq. (3.67) of [7])

$$\chi = \frac{2}{n\bar{g}_{\text{MS}}^2(1/L)} - \frac{(n-2)}{2\pi n} \gamma_2^{(2)}(\ell) - \frac{(n-2)}{2\pi^2 n} r_2(\ell) \bar{g}_{\text{MS}}^2(1/L) + \dots \quad (3.1)$$

where $\bar{g}_{\text{MS}}(q)$ is the minimal subtraction (MS) scheme running coupling at momentum scale q . The function $r_2(\ell)$ appearing above is given by (cf eq. (3.68) of [7])

$$r_2(\ell) = \bar{w}(\ell) - 2\kappa_{10}(\ell) - \frac{1}{2} \gamma_2^{(2)}(\ell) \left(\alpha_1^{(2)}(\ell) - \frac{1}{\ell} - \frac{1}{2} \gamma_2^{(2)}(\ell) \right) - \frac{(n-2)}{4\ell} \left(\gamma_3^{(2)}(\ell) + 1 \right), \quad (3.2)$$

where $\bar{w}(\ell)$ appears in the expansion of the sunset diagram defined (see (B.5)).

For large ℓ (cf (B.20), (B.25), (B.28)-(B.30) of [5]):

$$\alpha_1^{(2)}(\ell) \simeq \alpha_{1/2}^{(1)}(1) + \frac{\pi}{3} \ell - 2 + \frac{1}{\ell}, \quad (3.3)$$

$$\gamma_2^{(2)}(\ell) \simeq \alpha_{1/2}^{(1)}(1) - 2 + \frac{2\pi}{3} \ell, \quad (3.4)$$

$$\gamma_3^{(2)}(\ell) \simeq \alpha_{3/2}^{(1)}(1) - \frac{2}{3} + \frac{4\pi^2}{45} \ell^3. \quad (3.5)$$

The susceptibility computed from the simple rotator is given by (cf eq. (2.4) of [5]):

$$\chi_{\text{rot}} = \frac{2}{n\bar{g}_{\text{FV}}^2(L)} - \frac{(n-2)}{3n} \ell + \frac{(n-2)(n-4)}{90n} \ell^2 \bar{g}_{\text{FV}}^2(L) + \dots, \quad (d=2), \quad (3.6)$$

where \bar{g}_{FV} is the LWW running coupling [8] defined through the finite volume mass gap:

$$\bar{g}_{\text{FV}}^2(L) \equiv \frac{2}{n-1} L E_1(L). \quad (3.7)$$

Its expansion in terms of the running coupling in the MS scheme of DR is given by (cf eq. (2.2) in [8]):

$$\bar{g}_{\text{FV}}^2(L) = \bar{g}_{\text{MS}}^2(1/L) + c_1 \bar{g}_{\text{MS}}^4(1/L) + c_2 \bar{g}_{\text{MS}}^6(1/L) + \dots \quad (3.8)$$

The first two coefficients were computed in ref. [8]

$$c_1 = -\frac{(n-2)}{4\pi} Z, \quad (3.9)$$

$$c_2 = c_1^2 + \frac{c_1}{2\pi} + \frac{3(n-2)}{16\pi^2}, \quad (3.10)$$

where

$$Z \equiv \ln(4\pi) - \gamma, \quad (\gamma = -\Gamma'(1)). \quad (3.11)$$

The 3-loop coefficient c_3 can be obtained by combining Shin's 3-loop computation [9] of the finite volume mass gap using lattice regularization, with the computation of the 3-loop coefficient of the lattice beta-function by Caracciolo and Pelissetto [10].³ The result is given by

$$c_3 - 2c_1c_2 + c_1^3 = \frac{(n-2)}{(4\pi)^3} [S_2(n-2)^2 + S_1(n-2) + S_0], \quad (3.12)$$

with

$$S_0 = 64\pi^3 (s_1 + 2s_2 + 3s_3 - 0.02730084372483), \quad (3.13)$$

$$S_1 = 64\pi^3 (s_2 + 3s_3 - 0.00248186195281), \quad (3.14)$$

$$S_2 = 64\pi^3 (s_3 + 0.00004347976248), \quad (3.15)$$

where we have used Veretin's precise numerical values [13] of the lattice integrals appearing in the formulae, and the s_i are Shin's constants (appearing in eq. (2.25) of [9]) for which he quotes the following numerical values (in eqs. (2.28)–(2.30) of [9]):

$$s_1 = 0.02903(1), \quad (3.16)$$

$$s_2 = 0.000756(1), \quad (3.17)$$

$$s_3 = -0.000649(1). \quad (3.18)$$

Next we insert the expansion (3.8) in (3.6) and compare the resulting expression with the perturbative result given in (3.1). First we see that the $\bar{g}_{\text{MS}}^0(1/L)$ terms match for large ℓ if

$$\frac{(n-2)}{2\pi} \gamma_2^{(2)}(\ell) \simeq 2c_1 + \frac{(n-2)}{3} \ell. \quad (3.19)$$

This is satisfied since (using (3.4))

$$\alpha_{1/2}^{(1)}(1) = 2 - Z, \quad (3.20)$$

which is a special case of the general relation

$$\alpha_s^{(1)}(1) = \alpha_{1/2-s}^{(1)}(1) = \frac{1}{s(1-2s)} + 2\pi^{-s}\Gamma(s)\zeta(2s). \quad (3.21)$$

Matching at order $\bar{g}_{\text{MS}}^2(1/L)$ requires⁴

$$\bar{w}(\ell) - 2\kappa_{10}(\ell) \simeq \frac{2\pi^2}{45}\ell^2 - \frac{\pi}{6}Z\ell + \frac{3}{4} - \frac{Z}{2} + \frac{Z^2}{4} + \text{O}(1/\ell). \quad (3.22)$$

Using eq. (B.11) and the fact that $\kappa_{10}(\infty)$ is finite consistency requires

$$p_1 = 2\kappa_{10}(\infty) - \frac{\pi^2}{4} + \frac{1}{2} + \frac{1}{4}(Z-1)^2. \quad (3.23)$$

³Note that the original article ref. [10] had a few misprints, some of which were noticed by Shin [11]; the final correct result was first presented in ref. [12].

⁴Note the terms proportional to $(n-2)$ match.

Using

$$\kappa_{10}(\infty) = -0.024787427871346432238, \quad (3.24)$$

consistency is obtained if

$$p_1 = -1.789538253208505789488. \quad (3.25)$$

We arrive at the result

$$\frac{\chi - \chi_{\text{rot}}}{\chi} = \frac{(n-2)(n+1)}{16\pi^3\ell} \zeta(3) \bar{g}_{\text{MS}}^4(1/L) + \dots \quad (3.26)$$

On the other hand, from our considerations of the modified rotator (cf eq. (11.5) of [5]) we would expect

$$\frac{\chi - \chi_{\text{rot}}}{\chi} = -\frac{4}{\ell} \Phi_3 (n+1) \bar{g}_{\text{MS}}^4(1/L) + \dots \quad (3.27)$$

where Φ_3 is the leading coefficient in the perturbative expansion of $\Phi(L)$, assuming the expansion starting at order \bar{g}_{MS}^8 :

$$\Phi(L) = \sum_{r=3} \Phi_r \bar{g}_{\text{MS}}^{2r+2}(1/L). \quad (3.28)$$

Comparing (3.26) with (3.27) determines

$$\Phi_3 = -\frac{(n-2)}{(2\pi)^3} f_3 \quad (3.29)$$

with

$$f_3 = \frac{1}{8} \zeta(3) = 0.15025711290. \quad (3.30)$$

As a consequence, the low-lying spectrum to order \bar{g}_{MS}^8 is given by

$$\begin{aligned} LE_I(L) = \frac{1}{2} \mathcal{C}_{n;I} \bar{g}_{\text{MS}}^2(1/L) & \left\{ 1 + c_1 \bar{g}_{\text{MS}}^2(1/L) + c_2 \bar{g}_{\text{MS}}^4(1/L) \right. \\ & \left. + \bar{c}_3 \bar{g}_{\text{MS}}^6(1/L) + \dots \right\} + \mathcal{C}_{n;I}^2 \Phi_3 \bar{g}_{\text{MS}}^8(1/L) + \dots \end{aligned} \quad (3.31)$$

where

$$\bar{c}_3 = c_3 - 2(n-1)\Phi_3. \quad (3.32)$$

Hence we conclude, for example,

$$LE_1(L) - \frac{(n-1)}{2n} LE_2(L) = 2\pi(n^2-1)(n-2)f_3 \alpha_{\text{MS}}^4(1/L) + \dots, \quad (3.33)$$

where $\alpha_{\text{MS}} = \bar{g}_{\text{MS}}^2/(2\pi)$.

In the next subsection we test this prediction for $n=3$ and $n=4$ for which independent computations of the spectrum of excited states exist. The first computations for $O(3)$ were done by Balog and Hegedüs [3] using the TBA equations with the knowledge of the exact Zamolodchikov S-matrix [14]. Later Gromov, Kazakov and Vieira [6] computed the excited states for $O(4)$ from Hirota dynamics; in earlier papers Balog and Hegedüs [4, 15] computed the mass gap E_1 for $O(2r)$ but not E_2 .

3.1 Running coupling functions

For the perturbative analysis of their data, Balog and Hegedüs [4] introduced a function $\bar{g}_J^2(L)$ of the box size L ⁵ through

$$\frac{1}{\bar{g}_J^2(L)} + \frac{b_1}{b_0} \ln(b_0 \bar{g}_J^2(L)) = -b_0 \ln(\Lambda_{\text{FV}} L), \quad (3.34)$$

where b_0, b_1 are the universal first perturbative coefficients of the β -function:

$$b_0 = \frac{(n-2)}{2\pi}, \quad b_1 = \frac{(n-2)}{(2\pi)^2}, \quad (3.35)$$

and Λ_{FV} is the Λ -parameter of the LWW finite volume coupling in (3.7).

For $\Lambda_{\text{FV}} L$ small there are usually two solutions of (3.34) for $\bar{g}_J^2(L)$, one large and one small⁶. We chose the solution which is small for $\Lambda_{\text{FV}} L$ small, which has the property

$$\bar{g}_J^2(L) = \bar{g}_{\text{FV}}^2(L) + \mathcal{O}(\bar{g}_{\text{FV}}^6(L)), \quad \Lambda_{\text{FV}} L \ll 1. \quad (3.36)$$

It is appropriate to call \bar{g}_J a ‘‘running coupling function’’ since it satisfies the equation

$$L \frac{\partial}{\partial L} \bar{g}_J^2(L) = b_0 \bar{g}_J^4(L) \left[1 - \frac{b_1}{b_0} \bar{g}_J^2(L) \right]^{-1}, \quad (3.37)$$

i.e. like a perturbative running coupling with β -function coefficients $b_r = b_0 (b_1/b_0)^r$, $\forall r$.

Balog and Hegedüs consider \bar{g}_J^2 as a function of $z = ML$ where M is the infinite volume mass gap:

$$\frac{1}{\bar{g}_J^2(z)} + \frac{b_1}{b_0} \ln(b_0 \bar{g}_J^2(z)) = -b_0 \ln(z) + b_0 \ln(M/\Lambda_{\text{FV}}). \quad (3.38)$$

The ratio M/Λ_{FV} is known from the work of Hasenfratz and Niedermayer [17]⁷

$$\frac{M}{\Lambda_{\text{FV}}} = \frac{(8/e)^\Delta e^Z}{\Gamma(1+\Delta)}, \quad \Delta = \frac{1}{n-2}. \quad (3.39)$$

Defining $\alpha_J = \bar{g}_J^2/(2\pi)$ the equation becomes [4]

$$\frac{1}{\alpha_J(z)} + \ln(\alpha_J(z)) = -(n-2) \ln(z) + J(n), \quad (3.40)$$

with

$$J(n) = (n-2) [Z - \ln(\Gamma(1+\Delta))] - \ln(n-2) - 1 + \ln(8). \quad (3.41)$$

In particular,

$$J(3) = \ln(32\pi) - \gamma - 1, \quad J(4) = \ln(256\pi) - 2\gamma - 1. \quad (3.42)$$

⁵analogous constructions can be made for functions of lengths in infinite volume

⁶The solution of the equation $\frac{1}{\alpha} + \ln(\alpha) = -\ln(X)$ is $\alpha = -\frac{1}{W_{-1}(-X)}$, where $W_{-1}(z)$ is the Lambert W -function [16], first studied by Euler in 1783, and the index -1 refers to the real branch for which $\alpha \approx -1/\ln(X) \rightarrow +0$ when $X \rightarrow +0$.

⁷ $M/\Lambda_{\overline{\text{MS}}} = (8/e)^\Delta/\Gamma(1+\Delta)$ and $\Lambda_{\text{FV}}/\Lambda_{\text{MS}} = \exp\{-Z/2\} = \Lambda_{\text{MS}}/\Lambda_{\overline{\text{MS}}}$.

The LWW coupling has the following expansion in terms of \bar{g}_J^2 :

$$\bar{g}_{\text{FV}}^2 = \bar{g}_J^2 \{1 + (n-2)\alpha_J^2 + j_3\alpha_J^3 + \dots\}, \quad (3.43)$$

with the coefficient j_3 given by

$$j_3 = \frac{1}{8} \left\{ R_2(n-2)^3 + \left(R_1 - Z^2 + 4Z - \frac{1}{3} \right) (n-2)^2 + [R_0 + 6 + 6\zeta(3) + 4Z](n-2) - 2 - 6\zeta(3) \right\}, \quad (3.44)$$

where the constants R_i are given in (3.13)–(3.15). Inserting the numerical values (3.16)–(3.18) we obtain

$$j_3 = 1.195(4), \quad (n=3), \quad (3.45)$$

in agreement with the value quoted in eq. (4.4) of [3].

3.2 The Balog-Hegedüs results for the $I = 1, 2$ energies for $O(3)$

In table 1 we reproduce the data of Balog and Hegedüs [3]; ($f_{3,\text{est}}$ appearing in the last column is defined in (3.48)). Firstly we remark that by fitting the data for the mass gap E_1 one obtains a value of j_3 close to that given in (3.45) deduced from Shin's analysis.

Table 1. $O(3)$ energies for isospins $I = 1, 2$.

z	$\alpha_J(z)$	LE_1	LE_2	E_2/E_1	$f_{3,\text{est}}$
0.000001	0.05041270	0.31761386	0.95266912	2.9995	0.17707
0.000003	0.05354045	0.33744157	1.01210305	2.9993	0.17888
0.00001	0.05746199	0.36233411	1.08670379	2.9992	0.18159
0.00003	0.06159640	0.38862064	1.16546204	2.9990	0.18421
0.0001	0.06689778	0.42239721	1.26662427	2.9987	0.18785
0.0003	0.07263603	0.45905560	1.37636109	2.9982	0.19195
0.001	0.08023212	0.50775883	1.52204192	2.9976	0.19757
0.003	0.08877837	0.56282669	1.68656509	2.9966	0.20443
0.01	0.10066006	0.63994990	1.91651860	2.9948	0.21516
0.03	0.11489581	0.73342746	2.19419045	2.9917	0.23182
0.1	0.13647285	0.87841965	2.62093151	2.9837	0.27390
1.0	0.21988073	1.57045824	4.45605625	2.8374	0.72434

Secondly, from the fifth column of table 1, we see that although the ratio E_2/E_1 is close to the ratio of the Casimir eigenvalues, the data of Balog and Hegedüs establishes that the simple effective rotator model requires corrections.

We have for the $I = 2$ mass for $n = 3$ the expansion

$$LE_2(L) = 6\pi\alpha_J(z) \{1 + \alpha_J(z)^2 + (j_3 - 8f_3)\alpha_J(z)^3 + \dots\}, \quad (n=3). \quad (3.46)$$

With our value of f_3 we get a very small 3-loop coefficient

$$j_3 - 8f_3 = -0.007(4), \quad (n = 3), \quad (3.47)$$

which is similar to the remark in [3] (before their eq. (4.7)) that they numerically established that the 3-loop coefficient was zero. Although Shin's numbers (which have not yet been checked by an independent computation) are consistent with the data, to indicate whether or not $j_3 - 8f_3$ is non-zero would require the values of the s_i to a greater (at least a factor 10) accuracy than that obtained by Shin.

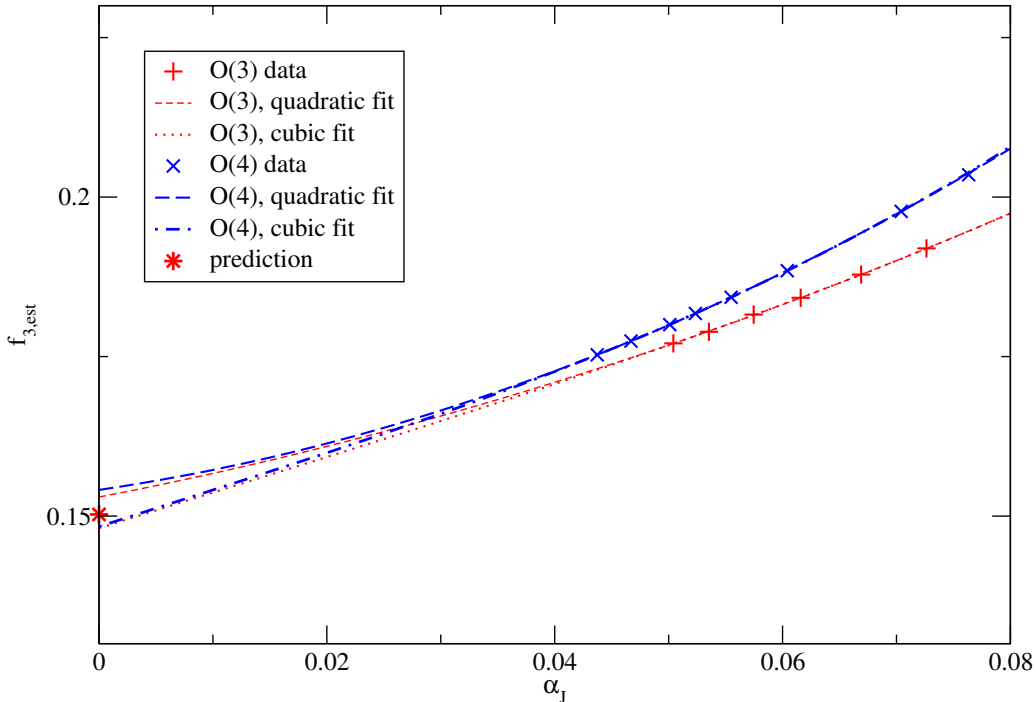


Figure 1. Plot of the estimates for f_3 given in (3.48) for $O(3)$ and $O(4)$. The curves are quadratic and cubic fits. The star indicates the prediction in (3.30) for $L \rightarrow 0$ limit.

To see even more clearly the agreement of our analysis with the data of Balog and Hegedüs, in fig. 1 we plot estimates for $f_{3,\text{est}}$ given by

$$f_{3,\text{est}} = \frac{1}{(n^2 - 1)(n - 2)2\pi\alpha_J^4} \left[LE_1(L) - \frac{(n - 1)}{2n} LE_2(L) \right], \quad (3.48)$$

for the case $n = 3$ (and for $n = 4$, see next subsection). Comparing the quadratic and cubic fits to the data in the range $0.05 < \alpha_J < 0.089$ (the first 8 points) one gets $f_3 = 0.151(2)$, which is in excellent agreement with our prediction in (3.30).

3.3 The $O(4)$ case

In [4] the 1-particle data for $z \geq 0.001$ for the $O(4)$ model is sufficiently precise for our purposes, however, the 2-particle results are missing. Gromov, Kazakov and Vieira [6] computed the 2-particle state energies, but for $z < 0.1$ we required higher precision than those

Table 2. $O(4)$ energies for isospins $I = 0, 1, 2$. The last column presents values of a 2-particle TBA parameter $\theta(z) = \theta_2(z) - \theta_1(z)$ discussed at the end of Appendix C.4

z	$L\mathcal{E}_0$	$L\mathcal{E}_1$	$L\mathcal{E}_2$	θ
0.0005	-1.358437256748	-0.944622579962	-0.255253656845	3.399048890
0.001	-1.3434090793	-0.9012815868	-0.164826477882	3.163405316
0.002	-1.325993755715	-0.8512533294	-0.060589525136	2.926136217
0.003	-1.31445222395	-0.818220925	0.008145288724	2.786480030
0.005	-1.29817998003	-0.771823922	0.104558415733	2.609523451
0.01	-1.27226343732	-0.6983802787	0.256829671226	2.367442907
0.03	-1.21827583735	-0.547406298	0.568266040311	1.9788498372
0.05	-1.185162243236	-0.456340311	0.754882156720	1.7962539024
0.1	-1.127336458694	-0.300410888	1.071796663945	1.5471797520
0.3	-0.9808905554557	0.07817485096	1.825340861386	1.1532273953
0.5	-0.87023469365833	0.35536400274	2.363197150958	0.9734482436
1.0	-0.64377457186332	0.938397059061	3.4676663603704	0.7385633684

presented in that reference. For $z \geq 0.1$ we used the data obtained using the Mathematica program in ref. [6]⁸.

Afterwards we have rewritten the code, discretizing the continuum formulation and using Fast Fourier Transform (FFT) to calculate the convolutions appearing. Due to FFT the calculation of an iterative step becomes much faster and yields more precise values. In addition, approximating the 1d continuum functions by a finite lattice of N points, and using several N values (typically $N = 2^{10} \dots 2^{14}$), one can get the continuum limit by determining numerically the coefficients of the corresponding $1/N$ expansion. Some details are given in Appendix C.

With this technique we could lower z , the size of periodic box down to $z = 0.0005$. For $z < 0.0005$ it becomes more time consuming to produce reliable estimates⁹, but the values of $\alpha_J(z)$ (see table 3) are already quite small.

Our data for the TBA energies \mathcal{E}_I for $I = 0, 1, 2$ is presented in table 2. The corresponding values for the excitation energies

$$E_I(L) = \mathcal{E}_I(L) - \mathcal{E}_0(L) \quad (3.49)$$

for isospins¹⁰, $I = 1, 2$ together with α_J are given in table 3.

In that table we see that Casimir scaling holds approximately for a large range of volumes. Also we show estimates for $f_{3,\text{est}}$ given by (3.48); which are plotted in fig. 1 together with quadratic and cubic fits. In the range $0.0437 < \alpha_J < 0.075$ (7 points)

⁸We thank Nikolay Gromov for sending these data to us.

⁹Note that with decreasing z the region of attraction shrinks, and it becomes more and more difficult to start the iterative method in the corresponding region.

¹⁰In the sector with a given isospin I only states with particle number $\nu \geq I$ contribute. Among these the $\nu = I$ is the lightest, and the TBA equations used describe just the $\nu = I = 1$ and the $\nu = I = 2$ states.

one gets $f_3 = 0.151(3)$. Like in the $O(3)$ case, this is consistent with our expected value $f_3 = 0.150257$ in (3.30).

Table 3. $O(4)$ excitation energies for isospins $I = 1, 2$.

z	$\alpha_J(z)$	LE_1	LE_2	E_2/E_1	$f_{3,\text{est}}$
0.0005	0.04373119	0.41381468	1.10318360	2.6659	0.17527
0.001	0.04669606	0.44212749	1.17858260	2.6657	0.17743
0.002	0.05010437	0.47474043	1.26540423	2.6655	0.18001
0.003	0.05234604	0.49623130	1.32259751	2.6653	0.18176
0.005	0.05548218	0.52635606	1.40273840	2.6650	0.18429
0.01	0.06041440	0.57388316	1.52909311	2.6645	0.18846
0.03	0.07041275	0.67086954	1.78654188	2.6630	0.19776
0.05	0.07633870	0.72881932	1.94004440	2.6619	0.20349
0.1	0.08627485	0.82692557	2.19913312	2.6594	0.21551
0.3	0.10919349	1.05906541	2.80623142	2.6497	0.25110
0.5	0.12497836	1.22559870	3.23343184	2.6382	0.28403
1.0	0.15648842	1.58217163	4.11144093	2.5986	0.35723

4 The case $d = 3$

From eqs. (3.54)–(3.57) and (3.72)–(3.74) of [7] the expansion of the susceptibility with DR is given, already in [2],

$$\chi = \frac{2\rho_s}{n} \left(1 + \frac{1}{\rho_s L} \tilde{R}_1 + \frac{1}{(\rho_s L)^2} \tilde{R}_2 + \dots \right), \quad (4.1)$$

with for $D = 3$:

$$\tilde{R}_1 = -\frac{(n-2)}{4\pi} \left(\gamma_2^{(3)}(\ell) - 2 \right), \quad (4.2)$$

and, (recall $\bar{W} = -L^{4-2D}\Psi$),

$$\begin{aligned} \tilde{R}_2 = 2(n-2) \left\{ \Psi(\ell) + \frac{1}{32\pi^2} \left(\gamma_2^{(3)}(\ell) - 2 \right) \left[2\alpha_1^{(3)}(\ell) - \gamma_2^{(3)}(\ell) - 2 - \frac{2}{\ell} \right] \right. \\ \left. + \frac{(n-2)}{32\pi^2\ell} \left(\gamma_3^{(3)}(\ell) + 2 \right) \right\}. \end{aligned} \quad (4.3)$$

We require the large ℓ behaviors of the shape functions which we take from eqs. (B.20) and (B.27) of [5]:

$$\alpha_1^{(3)}(\ell) \simeq \alpha_{1/2}^{(2)}(1) + \frac{1}{3}\pi\ell - 2 + \frac{1}{\ell}, \quad (4.4)$$

$$\gamma_2^{(3)}(\ell) \simeq \alpha_{1/2}^{(2)}(1) - 2 + \frac{2}{3}\pi\ell, \quad (4.5)$$

$$\gamma_3^{(3)}(\ell) \simeq \alpha_{3/2}^{(2)}(1) - \frac{2}{3} + \frac{4}{45}\pi^2\ell^3. \quad (4.6)$$

For the mass gap we have from eqs. (5.9)–(5.11) of [7] (setting $\hat{\ell} = 1$)

$$E_1 = \frac{(n-1)}{2\rho_s L^2} \left[1 + \frac{1}{\rho_s L} \tilde{\Delta}^{(2)} + \frac{1}{(\rho_s L)^2} \tilde{\Delta}^{(3)} + \dots \right], \quad (4.7)$$

with

$$\tilde{\Delta}^{(2)} = (n-2)LR(0), \quad (4.8)$$

$$\tilde{\Delta}^{(3)} = (n-2)L^2 \left[-2L^{4-2D}\bar{\Psi} + \frac{3}{4L^{D-1}}\bar{I}_{10:D-1} + (n-3)R(0)^2 \right], \quad (4.9)$$

where we have set the coefficients of the four-derivative couplings $l_1 = l_2 = 0$.

From eq. (3.16) of [18] for $D \sim 3$:

$$\bar{I}_{10:D-1} = -\frac{1}{2\pi L^{D-3}} \left[\frac{1}{D-3} - \frac{1}{2}\alpha_1^{(2)}(1) + \frac{1}{2} + \mathcal{O}(D-3) \right]. \quad (4.10)$$

So for $d = 3$

$$\tilde{\Delta}^{(3)} = (n-2) \left[-2q_1 + \frac{3}{16\pi} \left\{ \alpha_1^{(2)}(1) - 1 \right\} + (n-3)L^2 R(0)^2 \right], \quad (4.11)$$

the $1/(D-3)$ singularities canceling as they should.

For the rotator we get

$$\begin{aligned} \chi_{\text{rot}} = & \frac{2\rho_s}{n} \left\{ 1 - \frac{1}{\rho_s L} \left[\frac{\ell}{6}(n-2) + \tilde{\Delta}^{(2)} \right] \right. \\ & \left. + \frac{1}{(\rho_s L)^2} \left[\frac{\ell^2}{180}(n-2)(n-4) - \tilde{\Delta}^{(3)} + \tilde{\Delta}^{(2)2} \right] + \dots \right\}. \end{aligned} \quad (4.12)$$

The expressions for χ and χ_{rot} agree at 1-loop order up to terms vanishing exponentially with ℓ since (see eq. (5.10) of [18])

$$L^{D-2}R(0) = \frac{1}{4\pi} \int_0^\infty u^{-1/2} [S(u)^{D-1} - 1] \quad (4.13)$$

$$= \frac{1}{4\pi} \left(\alpha_{1/2}^{(D-1)}(1) - \frac{2(D-1)}{D-2} \right) \quad (4.14)$$

$$= \frac{1}{4\pi} \left(\alpha_{1/2}^{(2)}(1) - 4 \right) \quad \text{for } D = 3. \quad (4.15)$$

Then one can check, using eqs. (4.4)–(4.6) and (B.15), that at 2-loop χ and χ_{rot} differ only by terms which vanish as $\ell \rightarrow \infty$, and neglecting terms which vanish exponentially we obtain

$$\frac{\chi - \chi_{\text{rot}}}{\chi} = \frac{(n-2)(n+1)}{16\pi^2 \ell} \left(\alpha_{3/2}^{(2)}(1) + \frac{4}{3} \right) (\rho_s L)^{-2} + \dots \quad (4.16)$$

Suppose the spectrum is given by (2.13) and that $\Phi(L)$ has the expansion starting at order $(\rho_s L)^{-4}$:

$$\Phi(L) = \sum_{r=3} \Phi_r (\rho_s L)^{-r-1}, \quad (4.17)$$

then from our considerations of the modified rotator (cf eq. (11.5) of [5])

$$\frac{\chi - \chi_{\text{rot}}}{\chi} = -\frac{4}{\ell} \Phi_3(n+1)(\rho_s L)^{-2} + \dots \quad (4.18)$$

which determines

$$\Phi_3 = -\frac{1}{64\pi^2} \left[\alpha_{3/2}^{(2)}(1) + \frac{4}{3} \right] (n-2), \quad (d=3). \quad (4.19)$$

Nyfeler and Wiese [19] have investigated the histogram of the uniform magnetization for the spin 1/2 Heisenberg model on the honeycomb lattice in the cylindrical regime (see eqs. (3.9)–(3.12) and fig. 4.3). Having previously determined the low-energy constants ρ_s and c for this model in the cubical regime, they took the NLO formula for Θ and the standard rotator spectrum, to compare the cylindrical regime. The agreement seemed to be very good, but their statistical errors are too large to see signs of our predicted Casimir² term (or even the NNLO term in Θ). We are not aware of any other measurements of the spectrum of the $d=3$ $O(n)$ models.

5 Acknowledgements

We would like to thank Janos Balog, Nikolay Gromov and Uwe-Jens Wiese for useful correspondence.

A Spectrum of $O(3)$ rotator in $d=1$ at finite lattice spacing

The aim here is to illustrate that the energy levels at a given order of the lattice spacing are polynomials of $C_I = I(I+1)$, not only of I .

The eigenvalues of the transfer matrix are given by

$$\lambda_I(\epsilon) = \frac{1}{2\epsilon} \int_{-1}^1 dz e^{-(1-z)/(2\epsilon)} P_I(z), \quad (A.1)$$

where $P_I(z)$ are the Legendre polynomials. These are polynomials in $1-z$ with coefficients which are polynomials of C_I of order I :

$$P_I(z) = \sum_{n=0}^I (1-z)^n \frac{(-1)^n}{2^n (n!)^2} \prod_{k=0}^{n-1} (C_I - C_k). \quad (A.2)$$

In the continuum limit one should take $\epsilon \rightarrow 0$. Neglecting non-perturbative, exponentially small terms $\propto e^{-1/\epsilon}$, one obtains the expansion ¹¹

$$\lambda_I(\epsilon) \simeq \sum_{n=0}^I \frac{(-1)^n \epsilon^n}{n!} \prod_{k=0}^{n-1} (C_I - C_k). \quad (A.3)$$

¹¹Note that the summand vanishes for $n > I$ hence the upper limit of the sum could be extended to infinity.

For the energies one obtains

$$E_I(\epsilon) = -\frac{1}{\epsilon} \ln(\lambda_I(\epsilon)) = C_I(1 + \epsilon) - \frac{1}{3}C_I(C_I - 6)\epsilon^2 + \frac{5}{2}C_I^2 \left(1 - \frac{1}{3}C_I + \frac{1}{60}C_I^2\right) \epsilon^3 + \mathcal{O}(\epsilon^4). \quad (\text{A.4})$$

Here the coefficients of ϵ^n are indeed polynomials in C_I .

B The sunset diagram for $D \sim 2, 3, 4$ for large ℓ

The sunset diagram for the susceptibility is (cf. [18] (4.1) and (4.36))

$$\begin{aligned} \Psi(\ell, \hat{\ell}) &= -L^{2D-4} \overline{W} L^{2D-4} \int_{V_D} dx \ddot{G}(x) G^2(x) \\ &= -\frac{1}{48\pi^2(D-4)} \left(10 \ddot{g}(0; \ell, \hat{\ell}) - \frac{1}{\mathcal{V}_D}\right) - \frac{1}{16\pi^2} \overline{W}(\ell) + \mathcal{O}(D-4), \end{aligned} \quad (\text{B.1})$$

here we have reinstated $\hat{\ell}$, but since we are working with $\hat{\ell} = 1$ we have $\mathcal{V}_D = \ell \hat{\ell}^{D-4} = \ell$.

For the analogous diagram in the infinite strip one had (cf. eqs. (5.11) and (5.61) in [18])

$$\overline{\Psi}(\hat{\ell}) = -L^{2D-4} W = L^{2D-4} \int_{V_\infty} dx \ddot{R}(x) R^2(x) = -\frac{1}{48\pi^2(D-4)} 10 \ddot{R}(0; \hat{\ell}) - c_w + \mathcal{O}(D-4). \quad (\text{B.2})$$

Further, for $\ell \gg 1$ one has up to exponentially small corrections (cf. eq. (5.20) in [18])

$$\ddot{g}(0; \ell, \hat{\ell}) - \frac{1}{\mathcal{V}_D} \simeq \ddot{R}(0; \hat{\ell}). \quad (\text{B.3})$$

In Appendix (B.4) of ref. [5] we derived the relation

$$\frac{1}{16\pi^2} \overline{W}(\ell) - \frac{1}{180} \ell^2 + \frac{1}{12} \beta_1^{(3)}(1) \left(\ell + \frac{9}{2}\right) + \frac{1}{16\pi^2} \left(\frac{3}{2} \alpha_0^{(3)}(1) - 1\right) \frac{1}{\ell} \simeq c_w. \quad (\text{B.4})$$

B.1 Case $D \sim 2$

For $D \sim 2$ (setting $\hat{\ell} = 1$)

$$\Psi(\ell) = \frac{1}{8\pi^2} \left[\frac{1}{(D-2)^2} + \frac{r_\Psi(\ell)}{(D-2)} + \overline{w}(\ell) \right] + \mathcal{O}(D-2), \quad (\text{B.5})$$

with

$$r_\Psi(\ell) \equiv -\alpha_1^{(2)}(\ell) - \frac{1}{2} + \frac{1}{\ell} \quad (\text{B.6})$$

$$\simeq -\alpha_{1/2}^{(1)}(1) + \frac{3}{2} - \frac{\pi}{3} \ell. \quad (\text{B.7})$$

For the analogous diagram in the infinite strip

$$\overline{\Psi} = \frac{1}{8\pi^2} \left[\frac{1}{(D-2)^2} + \frac{p_0}{(D-2)} + p_1 \right] + \mathcal{O}(D-2). \quad (\text{B.8})$$

Using similar methods to that used to derive (B.4) we obtain for $D \sim 2$:

$$\begin{aligned} \Delta\Psi &\equiv \Psi(\ell) - \bar{\Psi} \\ &\simeq \frac{\ell^2}{180} + \frac{1}{16\pi^2} \left[\frac{3\pi}{2} \left(\alpha_1^{(1)}(1) + 1 \right) - \frac{3}{2\ell} \left(\alpha_{3/2}^{(1)}(1) + \frac{1}{3} \right) \right. \\ &\quad \left. - \frac{2\pi\ell}{3(D-2)} + \frac{\pi\ell}{3} \left(\alpha_{1/2}^{(1)}(1) - 2 \right) \right]. \end{aligned} \quad (\text{B.9})$$

Comparing this with (B.5) and (B.8) requires

$$p_0 = -\alpha_{1/2}^{(1)}(1) + \frac{3}{2} = Z - \frac{1}{2}, \quad (\text{B.10})$$

and

$$\bar{w}(\ell) - p_1 \simeq \frac{2\pi^2\ell^2}{45} - \frac{\pi\ell}{6}Z + \frac{\pi^2}{4} - \frac{3}{4\pi\ell}\zeta(3). \quad (\text{B.11})$$

B.2 Case $D \sim 3$

For $d = 3$ (setting $\hat{\ell} = 1$)¹²

$$\Psi(\ell) = -\frac{1}{16\pi^2}\bar{\mathcal{W}}(\ell), \quad (\text{B.12})$$

with values given in eq. (4.45) of ref. [18]

$$\bar{\mathcal{W}}(\ell) = \begin{cases} 2.12506105522294, & \text{for } \ell = 1, \\ 1.90198910547056, & \text{for } \ell = 2. \end{cases} \quad (\text{B.13})$$

For $D \sim 3$ $\bar{\Psi}$ has a singularity:

$$\bar{\Psi} = -\frac{3}{16\pi(D-3)} + q_1 + \mathcal{O}(D-3). \quad (\text{B.14})$$

Again using similar methods to that used to obtain (B.4), we can derive the expansion of $\Delta\Psi$ for $D \sim 3$ for large ℓ , and find that the expansion of $\Psi(\ell)$ large ℓ is given by:

$$\begin{aligned} \Psi(\ell) &\simeq -\frac{\ell^2}{180} + q_1 - \frac{3}{32\pi} \left[\alpha_1^{(2)}(1) - 1 \right] \\ &\quad - \frac{\ell}{48\pi} \left[\alpha_{1/2}^{(2)}(1) - 4 \right] + \frac{3}{32\pi^2\ell} \left[\alpha_{3/2}^{(2)}(1) + \frac{4}{3} \right]. \end{aligned} \quad (\text{B.15})$$

For the purposes of this paper we do not need the value of the constant q_1 appearing in eqs. (B.14) and (B.15). However we can easily obtain its numerical value from the lattice computation of the perturbative coefficients of the moment of inertia given in eq. (7.7) of [20]:

$$\theta_1 = 0.310373220693 (n-2), \quad (\text{B.16})$$

$$\theta_2 = -0.000430499941 (n-2). \quad (\text{B.17})$$

¹²There is a printing error in eq. (4.44) of ref. [18]; for $d = 3$, $\Psi = -L^2\bar{W}$.

These coefficients are simply related to the coefficients in (4.7) through

$$\theta_1 = -\tilde{\Delta}^{(2)}, \quad \theta_2 = -\tilde{\Delta}^{(3)} + \tilde{\Delta}^{(2)2}. \quad (\text{B.18})$$

Using eq. (4.11) and the numerical values

$$\alpha_{1/2}^{(2)} = 0.0997350799980441171545246633952, \quad (\text{B.19})$$

$$\alpha_1^{(2)} = 0.100879698927913998245389274826, \quad (\text{B.20})$$

we obtain

$$\theta_2 = [2q_1 + 0.149993826254627007174930112530] (n - 2). \quad (\text{B.21})$$

Combining this with eq. (B.17) we get

$$q_1 = -0.075212163098. \quad (\text{B.22})$$

As a check, using eqs. (B.19) and (B.20) and

$$\alpha_{3/2}^{(2)}(1) = 0.104412211554310173598670103056, \quad (\text{B.23})$$

we obtain, by comparing (B.15) with (B.13) at $\ell = 2$, the estimate $q_1 \approx -0.07521075$ which agrees with (B.22) to nearly 5 digits¹³.

C The equations for the lowest energy state in a finite volume for the vacuum, 1- and 2-particle sectors

We consider here the $SU(2) \times SU(2)$ principal chiral model which is equivalent to the $O(4)$ non-linear sigma model.

Al. and A. Zamolodchikov [14] proposed a self consistent exact S-matrix for the principal chiral models, which is built from the factors

$$S_0(x) = -i \frac{\Gamma(1 + ix/2)\Gamma(1/2 - ix/2)}{\Gamma(1 - ix/2)\Gamma(1/2 + ix/2)}. \quad (\text{C.1})$$

In the equations for $I = 0, 1, 2$ discussed below the following kernels occur.

$$S_p(x) = S_0(x + i/2), \quad (\text{C.2})$$

$$\begin{aligned} K_0(x) &= \frac{1}{2\pi i} \frac{d}{dx} (\ln(S_0(x)^2)) \\ &= \frac{1}{2\pi} [\Psi(1 + ix/2) + \Psi(1 - ix/2) - \Psi(1/2 + ix/2) - \Psi(1/2 - ix/2)], \end{aligned} \quad (\text{C.3})$$

$$K_m(x) = K_0(x - i/2), \quad (\text{C.4})$$

$$K_{pp}(x) = K_0(x + i). \quad (\text{C.5})$$

In the relations above it is assumed that x is real. Unlike the others, $K_{pp}(x)$ has a pole term $-i/(\pi x)$. Further, it satisfies the relation

$$K_{pp}(x) = - \left(K_0(x) - \frac{1}{\pi(1 - ix)} + \frac{i}{\pi x} \right). \quad (\text{C.6})$$

¹³For $d = 4$ the analogous estimate for c_w at $\ell = 2$ was correct to 7 digits.

Below we shall consider separately the cases of the ground states in the sectors $I = 0, 1, 2$.

The equations to be solved are clearly presented in ref. [4]; our discussion, however is based on the notations of ref. [6].

C.1 The iterative calculation of the vacuum energy

The finite-volume vacuum energy is defined through a single function $A(x)$, which is obtained by an iterative solution.

The initial function is chosen for convenience as

$$A^{(0)}(x) = A_{00}(x) \equiv -\exp(-z \cosh(\pi x)) . \quad (\text{C.7})$$

The iterative step with the input function $A^{(k)}(x)$ calculates the output function¹⁴ $\hat{A}^{(k)}(x)$ through the steps $A^{(k)}(x) \rightarrow r(x) \rightarrow f(x) \rightarrow \hat{A}^{(k)}(x)$. The auxiliary functions¹⁵ are defined below. The reason for using $\hat{A}^{(k)}$ for the output, is that the input of the next iteration, $A^{(k+1)}(x)$, will be modified to improve the convergence of the iterations.

After introducing

$$r(x) = \ln \left(\frac{A^{(k)}(x) - 1}{|A^{(k)}(x)| - 1} \right) , \quad (\text{C.8})$$

and $r_c(x) = r(x)^*$, the function $f(x)$ is given by

$$f(x) = (K_0 * r - K_{\text{pp}} * r_c)(x) - r_c(x) . \quad (\text{C.9})$$

Here ‘*’ denotes convolution. Due to the singularity of $K_{\text{pp}}(x)$ at $x = 0$ a Principal Value integral appears in (C.9) instead of an ordinary convolution, which is more difficult to deal with numerically.

One can circumvent this problem by introducing the function

$$\Phi(x) = \frac{i}{\pi} \left(\frac{1}{x+i} + \frac{1}{x-i\epsilon} \right) , \quad (\text{C.10})$$

which besides of the PV integral includes also the extra $-r_c(x)$ in (C.9). One obtains then a simpler relation with two convolutions only,

$$f(x) = (K_0 * (r + r_c))(x) + (\Phi * r_c)(x) . \quad (\text{C.11})$$

Finally, the output function of the iteration step is

$$\hat{A}^{(k)}(x) = A_{00}(x) \exp \left(f^{(k)}(x) \right) . \quad (\text{C.12})$$

The vacuum energy after k -th iteration is given by

$$\mathcal{E}_0^{(k)} = -M \int_{-\infty}^{\infty} dx \operatorname{Re}(r^{(k)}(x)) \cosh(\pi x) . \quad (\text{C.13})$$

¹⁴We denote the output of the iteration with \hat{A} since it could be different from the input of the next iteration.

¹⁵For intermediate quantities like $r(x)$, $f(x)$ we don’t write the iteration number k , except for clarity when they appear in the final answer.

To improve convergence one can use the well known trick which takes the input for the next iteration a linear combination

$$A^{(k+1)}(x) = \alpha \hat{A}^{(k)}(x) + (1 - \alpha)A^{(k)}(x), \quad (\text{C.14})$$

with a parameter $0 < \alpha \leq 1$. Note that the choice of the parameter α does not influence the fixed point (provided that the iteration converges), however, it affects the properties of the iteration step, like the speed of convergence or whether the initial function $A^{(0)}(x)$ is in the domain of attraction of the iterative process. One expects that increasing α increases the speed of convergence to the fixed point but decreases the convergence region. The latter could be crucial for small L (i.e. small z) since decreasing L also shrinks the domain of attraction.

For later use, note that the FT of $\Phi(x)$ is quite simple,

$$\tilde{\Phi}(p) = -2(\Theta(p) + e^p\Theta(-p)), \quad (\text{C.15})$$

where $\Theta(p)$ is the Heaviside step function. The function $\tilde{\Phi}(p)$ is continuous, but its first derivative has a finite jump at $p = 0$.

C.2 Using discrete FT

The discrete FT in Maple is defined as

$$g_F[k] = \text{FT}(g)[k] = \frac{1}{\sqrt{N}} \sum_{j=0}^{N-1} e^{-i2\pi kj/N} g[j], \quad (\text{C.16})$$

and its inverse

$$g[j] = \text{IFT}(g_F)[j] = \frac{1}{\sqrt{N}} \sum_{k=0}^{N-1} e^{i2\pi kj/N} g_F[k]. \quad (\text{C.17})$$

Here

$$\begin{aligned} x_j &= jdx, \quad (j = 0, \dots, N-1), & p_k &= k \frac{dp}{2\pi}, \quad (k = 0, \dots, N-1) \\ dx &= \frac{Q}{\sqrt{N}}, \quad \frac{dp}{2\pi} = \frac{1}{Q\sqrt{N}}, & dx \frac{dp}{2\pi} &= \frac{1}{N}, \\ \exp\left(2\pi i \frac{kj}{N}\right) &= \exp(ip_k x_j), & g(x_j) &= g[j], \quad \tilde{g}(p_k) \sim Q g_F[k]. \end{aligned} \quad (\text{C.18})$$

It is assumed that $g(x)$ is a periodic function with period $2X = Ndx$. Since the functions appearing here are decreasing fast for $|x| \rightarrow \infty$, for sufficiently large N one can consider the function to be periodic, $g(-X) = g(X) = 0$. To represent both the positive and negative x values in an array with indices $1 \leq j \leq N$, we choose N points with coordinates $[x_j, j = 1, \dots, N] = [0, 1, 2, \dots, N/2 - 1, -N/2, \dots, -2, -1]dx$.

For $N \rightarrow \infty$ the resolutions $1/dx$ and $1/dp$ both in the original x -space (which is here related to rapidity) and in p -space are proportional to \sqrt{N} . The (rapidity) cutoff is given by $X = Ndx/2 \propto \sqrt{N}$. Therefore the N behavior given in (C.18) for constant Q obeys

both requirements: for $N \rightarrow \infty$ one approaches the continuum limit and the infinite cutoff limit.

At this point Q is independent on N but otherwise arbitrary. Its value can be chosen to represent $A(x)$ and $\tilde{A}(p)$ by their corresponding discretizations equally well. The number of points in the interval Σ_x , the width of the function $|A(x)|$, is $\Sigma_x/dx \approx \sqrt{N}\Sigma_x/Q$. Similarly, for $\tilde{A}(p)$ the number of points in its relevant region in Fourier space is $\Sigma_p/dp \approx \sqrt{N}\Sigma_p Q/(2\pi)$. The value of Q is expected to be optimal when these two numbers are roughly equal, i.e. $Q^2 \approx 2\pi\Sigma_x/\Sigma_p$.

Further for the convolution one has

$$(g * h)(x) = \int dy g(x-y) h(y) = \int \frac{dp}{2\pi} \tilde{g}(p) \tilde{h}(p) e^{ipx} \sim Q \text{IFT}(g_F h_F)(x). \quad (\text{C.19})$$

Rewriting (C.11) by performing a discrete Fourier transformation one gets

$$\begin{aligned} f(x) &= Q \text{IFT}(K_{0F}(p)(r_F(p) + r_{cF}(p)))(x) \\ &\quad - 2 \text{IFT}([\Theta(p) + e^p \Theta(-p)] r_{cF}(p))(x). \end{aligned} \quad (\text{C.20})$$

(The factor Q appears only in the first term!)

C.3 N -dependence of the sums appearing in FT and the Euler-Bernoulli relation

Assuming that the function $g(x)$ is smooth for $x \neq 0$, and it has a jump in the first derivative, according to the Euler-Bernoulli relation one has

$$\begin{aligned} &\int_{-\infty}^{\infty} dx g(x) - a \sum_{n=-\infty}^{\infty} g(an) \\ &= -B_2 \frac{\delta g'(0)}{2!} a^2 - B_4 \frac{\delta g'''(0)}{4!} a^4 - B_6 \frac{\delta g^{(5)}(0)}{6!} a^6 - \dots - B_{2k} \frac{\delta g^{(2k-1)}(0)}{(2n)!} a^{2n} \\ &= -\frac{1}{12} \delta g'(0) a^2 + \frac{1}{720} \delta g^{(3)}(0) a^4 - \frac{1}{30240} \delta g^{(5)}(0) a^6 + \dots \end{aligned} \quad (\text{C.21})$$

where $\delta g^{(n)}(0) = g^{(n)}(+0) - g^{(n)}(-0)$ is the jump of the corresponding derivative at $x = 0$. Here a is the lattice spacing representing dx or dp .

In our case $a^2 \propto 1/N$; hence under the assumption mentioned above, the corresponding sums have a $1/N$ expansion with integer powers. One can calculate a quantity for several N values and determine from these the expansion coefficients¹⁶. The corresponding fits produce a very stable continuum extrapolation, often to ~ 12 digits.

It seems that it is better to use the naive non-improved sum, (appearing anyhow in the FT) whose $1/N$ behavior is known rather than an improved sum which has a more complicated (or even unknown) type of approach to the continuum limit. In [6] the authors took $\alpha = 1/2$.

¹⁶Allowing in the fit odd powers of $1/N^{1/2}$ it turns out indeed that the coefficient of $1/N^{3/2}$ is suppressed by a factor of $\sim 10^{-5}$.

C.4 The energy of the 1-particle sector

For the 1-particle sector the input of an iteration step consists of a function $A^{(k)}(x)$ and a number $\theta^{(k)}$. Within an iteration one has the chain $[A^{(k)}(x), \theta^{(k)}] \rightarrow r(x) \rightarrow f(x) \rightarrow [\hat{A}^{(k)}(x), \hat{\theta}^{(k)}]$, (cf. [6]). The $A^{(k)}(x) \rightarrow r(x) \rightarrow f(x)$ part is given by the same expressions we had in (C.8) - (C.11).

In [6] the authors choose a general $\theta^{(0)}$ as a starting point of iterations. However, one can verify that $\theta^{(k)} \rightarrow 0$ for $k \rightarrow \infty$. The physical reason is that θ is related to the rapidity of the particle [4].¹⁷

The state in the $I = 1$ sector with the smallest energy is the 1-particle state with zero momentum, corresponding to $\theta = 0$. Starting the iteration with $\theta^{(0)} = 0$ all the subsequent $\theta^{(k)}$ values remain automatically zero. For this reason, we set $\theta = 0$, simplifying the iteration steps to $A^{(k)}(x) \rightarrow \hat{A}^{(k)}(x)$.

The output function after one iteration (for $\theta = 0$) is written in the form

$$\hat{A}^{(k)}(x) = A_{00}(x) [S_p(x)]^2 \exp(f^{(k)}(x)), \quad (\text{C.22})$$

(cf. (C.2)). The iteration $A^{(k)}(x) \rightarrow \hat{A}^{(k)}(x)$ has the same form as for the vacuum, given by (C.8)–(C.12). (Note that due to the factor $[S_p(x)]^2$ the agreement is only formal.)

Introducing the averaging in this case, one obtains for the next input function

$$A^{(k+1)}(x) = \alpha \hat{A}^{(k)}(x) + (1 - \alpha) A^{(k)}(x). \quad (\text{C.23})$$

The energy of the ground state in the 1-particle sector for $\theta = 0$ after the k -th iteration is given by

$$\mathcal{E}_1^{(k)} = M - M \int dx \operatorname{Re} \left(r^{(k)}(x) \right) \cosh(\pi x). \quad (\text{C.24})$$

C.5 The ground state energy of the 2-particle sector

For the case of the 2-particle sector, the input of an iteration step consists of a function $A^{(k)}(x)$ and two numbers, $\theta_1^{(k)}$ and $\theta_2^{(k)}$. In this case again it is enough to restrict the iteration to the zero total momentum, i.e. $\theta_1 + \theta_2 = 0$. (The iteration would drive the system anyhow to satisfy this condition at the FP.)

In the rest frame one has $\theta_2 = -\theta_1 = \theta/2$, where θ is related to the rapidity difference. Because of the symmetry $\theta \rightarrow -\theta$ we can restrict the discussion to $\theta > 0$.

In the case of zero total momentum the input of the iteration is $[A^{(k)}(x), \theta^{(k)}]$ and the output is $[\hat{A}^{(k)}(x), \hat{\theta}^{(k)}]$.

Consider the equation

$$z \sinh \left(\frac{1}{2} \pi \theta \right) + \operatorname{Im} \left[\ln (S_0^2(\theta)) + 2\phi \left(\frac{1}{2} \theta \right) \right] = 0, \quad (\text{C.25})$$

where we introduced the function (depending implicitly on the input variables)

$$\phi(x) = (K_m * r)(x). \quad (\text{C.26})$$

¹⁷In the expression of the energy [6] for general θ the first term in (C.24) is replaced by $M \cosh(\pi\theta)$. Note that the second term will also depend on θ through $r^{(k)}(x) = r^{(k)}(x; \theta)$.

The output value of θ is given by the positive solution of (C.25),

$$\hat{\theta}^{(k)} = \theta > 0. \quad (\text{C.27})$$

The output function $\hat{A}^{(k)}(x)$ after the k -th iteration is given by

$$\hat{A}^{(k)}(x) = A_{00}(x) \left[S_p \left(x + \frac{1}{2}\theta^{(k)} \right) S_p \left(x - \frac{1}{2}\theta^{(k)} \right) \right]^2 \exp(f^{(k)}(x)), \quad (\text{C.28})$$

where the procedure to obtain $f^{(k)}(x)$ is formally the same as for the $\nu = 0, 1$ cases. Here one can introduce two averaging parameters α_A and α_θ :

$$A^{(k+1)}(x) = \alpha_A \hat{A}^{(k)}(x) + (1 - \alpha_A)A^{(k)}(x). \quad (\text{C.29})$$

and

$$\theta^{(k+1)} = \alpha_\theta \hat{\theta}^{(k)} + (1 - \alpha_\theta)\theta^{(k)}. \quad (\text{C.30})$$

The presence of these two parameters plays an important role in the stability of the iteration and for the speed of convergence. For example, choosing $\alpha_\theta \ll 1$ the value of θ barely changes. In our O(4) simulations at small z we found that it is much easier to find a good starting point, (one in the domain of attraction of the fixed point) when one chooses $\alpha_\theta < \alpha_A$. For our last point, $z = LM = 0.0005$ we took $\alpha_A = 0.4$, $\alpha_\theta = 0.14$.

The energy of the ground state in the 2-particle sector after the k -th iteration is

$$\mathcal{E}_2^{(k)} = 2M \cosh \left(\frac{1}{2}\pi\theta^{(k)} \right) - M \int dx \operatorname{Re} \left(r^{(k)}(x) \right) \cosh(\pi x). \quad (\text{C.31})$$

For a given z and N we let the iteration run until the result stabilized (apart from fluctuations due to finite precision) yielding the FP value $\theta^{(\infty)}(N; z) = \lim_{k \rightarrow \infty} \theta^{(k)}(N; z)$ for several N values. (We used $N = 2^{10}, \dots, 2^{14}$). With these one can calculate the first few coefficients of the $1/N$ expansion, $\theta^{(\infty)}(N; z) = \theta(z) + t_1(z)/N + t_2(z)/N^2 + \dots$. This gives $\theta = \theta(z) = \theta_2(z) - \theta_1(z)$ appearing in (C.25) and tabulated in Table 2.

From the numerical analysis described above we found that $\theta(z)$ has a logarithmic dependence for small z , $\theta(z) \approx -\ln(z)/\pi + a$, where $a \simeq 1.0$.

Using the running coupling $\bar{g}_J^2(z)$ (cf. (3.34), (3.40)) one obtains a good fit (with an error smaller than 10^{-3}),

$$\theta(z) \approx \frac{1}{\bar{g}_J^2(z)} + A + B \bar{g}_J^2(z), \quad (\text{C.32})$$

where $A = -0.1754$, $B = -0.2385$.

As mentioned earlier, the domain of attraction seems to shrink with decreasing z , therefore it is important to choose a proper starting value $\theta^{(0)}$ for the iteration. The value obtained by (C.32) can be used for $\theta^{(0)}$. Note, however, that we did not investigate systematically questions related to the domain of attraction.

References

- [1] H. Leutwyler, *Energy Levels of Light Quarks Confined to a Box*, Phys. Lett. B **189** (1987) 197.
- [2] P. Hasenfratz and F. Niedermayer, *Finite size and temperature effects in the AF Heisenberg model*, Z. Phys. B92 (1993) 91.
- [3] J. Balog and A. Hegedus, *The finite size spectrum of the 2-dimensional $O(3)$ nonlinear sigma-model*, Nucl. Phys. B829 (2010) 425.
- [4] J. Balog and A. Hegedus, *TBA Equations for excited states in the $O(3)$ and $O(4)$ nonlinear sigma model*, J. Phys. A37 (2004) 1881.
- [5] F. Niedermayer and P. Weisz, *Isospin susceptibility in the $O(n)$ sigma-model in the delta-regime*, JHEP 1706 (2017) 150.
- [6] N. Gromov, V. Kazakov and P. Vieira, *Finite Volume Spectrum of 2D Field Theories from Hirota Dynamics*, JHEP 0912 (2009) 060.
- [7] F. Niedermayer and P. Weisz, *Matching effective chiral Lagrangians with dimensional and lattice regularizations*, JHEP 1604 (2016) 110.
- [8] M. Lüscher, P. Weisz and U. Wolff, *A Numerical method to compute the running coupling in asymptotically free theories*, Nucl. Phys. B359 (1991) 221.
- [9] D-S. Shin, *A Determination of the mass gap in the $O(n)$ sigma model*, Nucl.Phys. B496 (1997) 408.
- [10] S. Caracciolo and A. Pelissetto, *Four loop perturbative expansion for the lattice n vector model*, Nucl.Phys. B455 (1995) 619.
- [11] D-S, Shin, *Correction to four loop RG functions in the two-dimensional lattice $O(n)$ sigma model*, Nucl. Phys. B546 (1999) 669.
- [12] B. Alles, S. Caracciolo, A. Pelissetto and M. Pepe, *Four-loop contributions to long distance quantities in the two-dimensional nonlinear sigma model on a square lattice: Revised numerical estimates*, Nucl.Phys. B562 (1999) 581.
- [13] O. Veretin, *Analytical results for the four-loop RG functions in the 2D non-linear $O(n)$ σ -model on the lattice*, Phys. Part. Nucl. 44 (2013) 573.
- [14] Alexander B. Zamolodchikov and Alexei B. Zamolodchikov, *Relativistic Factorized S Matrix in Two-Dimensions Having $O(N)$ Isotopic Symmetry*, Nucl. Phys. B133 (1978) 525.
- [15] J. Balog and A. Hegedus, *TBA equations for the mass gap in the $O(2r)$ non-linear sigma-models*, Nucl. Phys. B725 (2005) 531.
- [16] See e.g. https://en.wikipedia.org/wiki/Lambert_W_function.
- [17] P. Hasenfratz and F. Niedermayer, *The Exact mass gap of the $O(N)$ sigma model for arbitrary $N \geq 3$ in $d = 2$* , Phys. Lett. B245 (1990) 529.
- [18] F. Niedermayer and P. Weisz, *Massless sunset diagrams in finite asymmetric volumes*, JHEP 1606 (2016) 102.
- [19] M. Nyfeler, *Numerical Simulations of Strongly Correlated Electron Systems on Bipartite and on Frustrated Lattices*, PhD. thesis 2009, http://www.wiese.itp.unibe.ch/theses/nyfeler_phd.pdf

- [20] F. Niedermayer and C. Weiermann, *The rotator spectrum in the delta-regime of the $O(n)$ effective field theory in 3 and 4 dimensions*, Nucl. Phys. B842 (2011) 248.